On the Mobilization of Metals by CO_2 Leakage into Shallow Aquifers: Exploring Release Mechanisms by Modeling Field and Laboratory Experiments

Liange Zheng [a], Nicolas Spycher [a], Charuleka Varadharajan, Ruth M. Tinnacher[a], John D. Pugh[b], Marco Bianchi [a], Jens Birkholzer [a], Peter S. Nico [a], and Robert C. Trautz [c]

[a] *Lawrence Berkeley National Laboratory, Berkeley, Califonia 94720, USA*
[b] *Southern Company Services, 600 N. 18th St., Birmingham, Alabama 35291, USA*
[c] *Electric Power Research Institute, 3420 Hillview Avenue, Palo Alto, California 94304, USA*

Abstract

The dissolution of CO_2 in water leads to a pH decrease and carbonate content increase in affected groundwater, which in turn can drive the mobilization of metals from sediments. The mechanisms of metal release postulated in various field and laboratory studies often differ. Drawing primarily on previously published results, we examine contrasting metal mobilization behaviors at two field tests and in one laboratory study, to investigate whether the same mechanisms could explain metal releases in these different experiments. Numerical modeling of the two field tests reveals that fast Ca-driven cation exchange (from calcite dissolution) can explain the release of most major and trace metal cations at both sites, and their parallel concentration trends. The dissolution of other minerals reacting more slowly (superimposed on cation exchange) also contributes to metal release over longer time frames, but can be masked by fast ambient groundwater velocities. Therefore, the magnitude and extent of mobilization depends not only on metal-mineral associations and sediment pH buffering characteristics, but also on groundwater flow rates, thus on the residence time of CO_2-impacted groundwater relative to the rates of metal-release reactions. Sequential leaching laboratory tests modeled using the same metal-release concept as postulated from field experiments show that both field and laboratory data can be explained by the same processes. The reversibility of metal release upon CO_2 degassing by de-pressurization is also explored using simple geochemical models, and shows that

the sequestration of metals by resorption and re-precipitation upon CO_2 exsolution is quite plausible and may warrant further attention.

Keywords: groundwater, carbonic acid, leak, CO_2 sequestration, CCS, CCUS

1. Introduction

CO_2 emissions from the burning of fossil fuels have become a serious concern because of their impact on climate. As a result, CO_2 capture followed by geologic storage (CCS) into deep saline aquifers is considered an important potential mitigation measure for climate change. Over the last decade, many studies have been undertaken to assess the feasibility and safety of CO_2 geologic storage, with an emphasis primarily on hydrological, geochemical, and mechanical processes affecting deep injection and containment in storage reservoirs. A smaller number of studies have been undertaken to assess the impacts of potential CO_2 leakage from deep storage reservoirs on the quality of overlying freshwater aquifers (see review papers Lemieux[1] and Harvey et al.[2], and references therein). Observations from these studies are summarized below, and provide background to evaluations presented later about the chemical processes potentially responsible for observed mobilization of metals at two field sites previously investigated by the authors.

1.1 Observations from laboratory experiments

Due to their low cost and relative ease of operation, several laboratory batch and column experiments have been conducted to investigate the mobilization of trace elements in response to CO_2 intrusion into potable groundwater. Typically, these experiments[3-11] have involved the release of CO_2 into a pre-equilibrated water-rock environment, followed by monitoring of the geochemical changes in the aqueous phase.

Smyth et al.[3] and Lu et al.[4] presented laboratory batch experiments exposing aquifer materials from the Texas Gulf Coast region to elevated levels of CO_2. Two different types of responses were

observed in these studies: “Type I cations” (Ca, Mg, Si, K, Sr, Mn, Ba, Co, B, Zn) displayed a rapidly increasing concentration at the start of CO_2 injection that became steady before the end of the experiment, whereas “Type II cations” (Fe, Al, Mo, U, V, As, Cr, Cs, Rb, Ni and Cu) showed an initial concentration increase at the start of CO_2 injection, followed by a decrease to values lower than levels prior to injection. Little and Jackson[5] performed laboratory experiments of CO_2 infiltration for more than 300 days on samples from different freshwater aquifers. While increases in the concentration of alkali and alkaline earth metals were quite consistent in most of their experiments, increases in trace element concentrations were observed only in some samples. Wei et al.[6] reacted gaseous CO_2 with soil sampled in the vadose zone, at a depth around 0.1 m below the surface for three days, and observed increases in Mg, K, Al, Cr, Mn, Fe and Pb concentrations ranging from 50% to 500%, depending on the metal and moisture content of the soil. Their study demonstrates that CO_2 leakage could mobilize trace metals not only from an aquifer, but also from the vadose zone. Viswanathan et al.[7] conducted a batch experiment to specifically test the leaching out of As from samples collected at the Chimayo, New Mexico, natural analogue site, aiming to shed light on the high concentrations of As observed in a few wells with elevated levels of natural CO_2 [12]. They observed a sharp increase of As concentrations as soon as pH dropped, but then a slow decrease in concentrations (although pH remained low, suggesting that H-driven desorption leads to the release of As). Humez et al.[8] conducted a water-mineral-CO_2 batch experiment with samples taken from the Albian aquifer in the Paris Basin (France). They observed an increase in concentrations of Ca, Si, Na, Al, B, Co, K, Li, Mg, Mn, Ni, Pb, Sr, Zn, a decline in Fe and Be concentrations, and no changes for Cl and SO_4 after initial CO_2 influx. Varadharajan et al.[9] conducted a series of sequential leaching tests with sediments from a shallow groundwater formation in Mississippi, USA. Constituents that were mobilized were As, Ba, Ca, Fe, Ge, Mg, Mn, Na, Ni, Si, Sr, Zn, which are largely consistent with the Type I cations reported by Lu et al. (2010). Wunsch et al.[10] reacted rock samples from three limestone aquifers with 0.01–1 bar CO_2

for up to 40 days, and found increasing concentrations of Ca, Mg, Sr, Ba, Tl, U, Co, As and Ni from the dissolution of mostly calcite and to a lesser extent pyrite. Researchers from the same group (Kirsch et al.[11]) reacted sandstone samples with CO_2 under similar conditions for 27 days, showing a rapid increase in major (Ca, Mg) and trace (As, Ba, Cd, Fe, Mn, Pb, Sr, U) elements, which was attributed to the dissolution of calcite.

Together, these experiments analyzed various types of sediments (e.g., essentially carbonate-free in Varadharajan et al.[9] vs. carbonate-dominated in Wunsch et al.[10]) in a variety of conditions in terms of redox state (e.g., reducing in Varadharajan et al.[9] vs. oxidizing in Little and Jackson[5]), pressure conditions (e.g., 4 bars in Varadharajan et al.[9] vs. atmospheric pressure in most batch experiments, e.g., Humez et al.[8]), and reaction times ranging from a couple days [6], tens of days[8-11] to hundreds of days. [5] Although this wide range of experimental conditions with various sediment types resulted in different dissolved metal concentration responses, one common observation found in these experiments was the rapid increase in alkali and alkaline earth metals, including Na, K, Ca, Mg, Sr and Ba. As will be discussed later in this paper, these increases, often displaying parallel concentration trends, could be explained by ion exchange.

1.2 Observations from field tests

Although laboratory experiments facilitate the understanding of the potential impact of CO_2 on groundwater, they cannot accurately represent *in situ* conditions. For example, pre-equilibration of synthetic solutions[3] or DI water[4] with sediments, unwanted oxidation during the experiment[5], or neglecting the transport of groundwater and CO_2 can lead to laboratory conditions that do not adequately represent field conditions. Field tests are therefore desirable, even though experimental conditions in the field cannot be controlled as tightly as in the laboratory. Several fields test have been conducted recently. Peter et al.[13] reported on a field site where CO_2 was injected through three wells for a period of 10 days into an aquifer at a depth of 18 m in Northeast Germany. Water

samples from downgradient monitoring wells showed a moderate increase in Ca, K, Mg and Fe (~15% to 40%), and a significant increase in Al, Si, Mn (~120% to 180%) in comparison with baseline groundwater. An increase in the dissolved concentrations of heavy metals was also noted. Gahill and Jakobsen[14] also reported a field scale pilot test in which CO_2 gas was injected at 5-10 m depth into an unconfined aquifer in Denmark for two days, with monitoring of water geochemistry for more than 100 days. In addition to a one-unit drop in pH and a two-fold increase in electrical conductivity (EC), increases in major and trace element concentrations were ~260% and 320% for Ca and Mg, respectively, ~50% for Na and Si, as well as ~730%, 370%, 330% and 160% for Al, Ba, Sr, and Zn respectively.

Groundwater quality was also monitored at the CO_2-Field Lab test site in Southern Norway[15]. This test consisted of a 6-day injection of CO_2 into a shallow glacio-fluvial aquifer at a depth of 20 m, followed by about a week of post-injection monitoring at various depths using multiple observation wells. A significant increase in dissolved Ca and Si concentration was observed at some locations, in addition to a strong pH drop and alkalinity increase. However, the sediment heterogeneity and mixing of seawater with fresh water at this site complicated the interpretation of the test results. Most recently, a single-well push-pull test was conducted in a shallow aquifer at Cranfield, Mississippi[16]. In this case, the mobilization and/or retardation of major and trace elements were quantified using a mixing model to evaluate the concentration trends observed during the test. Although mobilization of major cations and most trace metals was confirmed by this field test, the observed changes in the dissolved concentrations of major and trace elements could not be used to pinpoint CO_2 leakage because of the wide spatiotemporal variability in background groundwater compositions at the test site. The ZERT (Zero Emissions Research and Technology) field test in Montana, USA,[17,18] and a field test conducted in Mississippi[19] are two other field experiments that revealed the mobilization of dissolved metals upon introduction of

132 CO_2 into groundwater. These two tests are the focus of this paper and will be discussed later in
133 more details.

134 In general, observations from both field and laboratory experiments show an increase in the
135 dissolved concentrations of major and trace elements upon CO_2 release. However, there appears to
136 be two noticeable differences between the results of field and laboratory tests. First, the rise in
137 concentrations of dissolved constituents observed during field tests is typically much less
138 pronounced than in laboratory experiments— field tests show increases of about an order of
139 magnitude or less, compared to levels prior to CO2 injection (20% to 700% in the studies cited
140 above), whereas orders-of-magnitude increases have been observed in laboratory tests. Second,
141 increases in trace element concentrations, especially those of environmental relevance such as As,
142 Pb, Ba, and Cd, are more frequently reported in laboratory tests than in field tests. Potential
143 reasons for these differences are investigated in the present study.

144

145 **1.3 Objectives of present study**

146 In this paper, we use numerical models to investigate two issues regarding the impact of CO_2
147 leakage into groundwater: 1) the chemical processes leading to the mobilization of metals and 2)
148 the potential reversibility of these processes upon CO_2 exsolution, which would occur if deep CO_2-
149 saturated groundwater migrated (or was pumped) to shallow depths. Our objectives are first to
150 compare previous and new modeling results for two different field tests and one laboratory study,
151 to determine whether the same mechanisms could explain the mobilization of metals in these
152 experiments. Another objective is to bring up the subject of metal release reversibility, which has
153 not been given much attention in the literature. Our investigations on revesibility are limited to the
154 use of simple models to illustrate the concept, with the goal to stimulate interest in this topic for
155 further studies.

Numerical models have been used to perform generic evaluations of the potential impact of CO_2 leakage on the water quality of shallow aquifers,[20-24] to identify potential issues such as the leaching out of organic compounds at depth by supercritical CO_2 and their release in shallow aquifers,[25] and to interpret laboratory experiments,[7,10,11] as well as field tests,[19,26] to understand the underlying transport and chemical processes that control the mobilization of major and trace elements upon CO_2 dissolution in groundwater. By integrating modeling efforts with real data sets from field and laboratory experiments, conceptual models of metal release can be tested, and their application to different field settings and/or experimental conditions can be evaluated.

Here, we examine the contrasting metal-mobilization behavior at the Montana State University-Zero Emissions Research and Technology (MSU-ZERT) field test in Montana, [17] and a field test conducted in Plant Daniel, Mississippi [19], with the goal to advance our understanding of water-quality changes that may occur due to CO_2 intrusion/influx under different hydrologic and geochemical settings. We compare results of previous and new modeling investigations by our group at the field scale. We then also model sequential leaching laboratory tests performed on sediments collected at the site in Mississippi[9] to evaluate whether the metal-release concepts developed based on the field data is consistent with the laboratory study.

2. Reactive Processes

As postulated on the basis of laboratory tests,[4] and revealed through simulations of laboratory experiments[7,8,10,11] and field tests, [19,26] the chemical processes leading to the release of metals in aquifers impacted by CO_2 can be summarized as follows. The dissolution of CO_2 in water produces carbonic acid, which decreases pH and increases the dissolved carbonate content in impacted groundwater:

$$CO_{2(g)} + H_2O = H_2CO_{3(aq)} \quad (1)$$

$$H_2CO_{3(aq)} = HCO_3^- + H^+ \quad (2)$$

In pure water, the dissolution of CO_2 at pressure > 5 bars yields a pH near 3.5; however, in natural systems the pH drop is not as pronounced (values typically near or above 5) because of buffering by various reactions. For example, at the Frio deep CO_2 injection test site,[27] injection of supercritical CO_2 at pressures ~150 bar into a deep sandstone aquifer resulted in pH dropping from about 6.5 to 5.7. Under totally different conditions in shallow sandy gravels, a few meters below the ground surface at the MSU-ZERT site, [17] the pH decreased from around 7 to 6 after injection of gaseous CO_2 through a horizontal pipe at 2-2.3 m deep. A more significant pH decrease, from about 8 to 5.1, was observed at the Mississippi site[19] upon injection of groundwater carbonated at pressure near 4 bar into a confined, poorly buffered formation predominantly containing sandy sediments.

The decrease in groundwater pH upon carbonation can release metals (M) by the dissolution of minerals, most particularly carbonates and sulfides:

$$MCO_{3(s)} + H^+ \rightarrow M^{2+} + HCO_3^- \quad (3)$$

$$MS_{(s)} + H^+ \rightarrow M^{2+} + HS^- \quad (4)$$

Adsorption-desorption reactions are also expected to play an important role in metal mobilization, and also in buffering pH in the absence of significant amounts of fast-reacting carbonate minerals:

$$>SOM^+ + H^+ \rightarrow >SOH + M^{+2} \quad (5)$$

$$>SOH + H^+ \rightarrow >SOH_2^+ \quad (6)$$

Competitive sorption with bicarbonate ions (e.g., As, Se) could also release metal oxyanions:

$$>SMO_4^{-n} + HCO_3^- \rightarrow >SHCO_3^- + MO_4^{-n} \quad (7)$$

In addition, metals released by the above reactions (e.g., Ca) may trigger exchange reactions that then cause the further release of other metals into solution:

$$X\text{-}M + Ca^{+2} \rightarrow X\text{-}Ca + M^{+2} \quad (8)$$

These reactive processes were investigated by numerical modeling at both the MSU-ZERT[26] and Mississippi test sites, [19] as discussed below.

206 **3. Modeling Interpretations of Field Tests**

207 In the MSU-ZERT field experiment,[17] gaseous CO_2 was injected for about one month into a
208 horizontal pipe located about a meter below the water table of a very shallow freshwater aquifer,
209 under natural (steep) hydraulic gradient conditions. Sediments beneath this site consisted primarily
210 of Cenozoic alluvial sandy gravel deposits. The groundwater composition was monitored prior to,
211 during, and (for about a week) following injection. Rain fell on several occasions over this shallow
212 test site, leaving a relatively small time window (about 10 days) during which the groundwater
213 composition was unaffected by rainfall during injection.[17]

214 The second study was conducted in Mississippi[19] (hereafter referred to as the Mississippi site).
215 This field test was driven in part by the need for an experiment over longer time frames, under
216 better geochemically constrained conditions, and into a deeper (~50 m) geologic formation than at
217 the MSU-ZERT site. The sediments at this test site consist primarily of Cenozoic deltaic/near-
218 shore marine, poorly consolidated sands interbedded with clays. In this experiment, groundwater
219 from a confined hydrostratigraphic interval was pumped and carbonated above ground, then re-
220 injected into the same interval (in a dipole, closed loop system) to simulate leakage of CO_2 from a
221 deep storage reservoir into an overlying aquifer. Injection of carbonated groundwater at this site
222 lasted for about 5 months, preceded by an extensive monitoring period of background conditions
223 (13 months, including 2 months of pumping without carbonation) and followed by a post-injection
224 monitoring period of about 10 months.

225 In both studies, the groundwater quality was monitored using dedicated monitoring wells
226 installed up- and downgradient from the injection location (groundwater samples for analyses of
227 trace metals were filtered, prior to acidification, at 0.1 μm in the MSU-ZERT test and 0.2 μm in
228 the Mississippi experiment, to minimize possible colloidal materials). Sediments at both sites were
229 also characterized to determine metal-sediment associations and to help understand key reactive
230 processes resulting from carbonation of the groundwater. Results from both these studies indicated

231 a significant pH decrease upon carbonation (by ~0.8 pH units at the MSU-ZERT site, and ~3 pH
232 units at the Mississippi site), accompanied by the release of primarily alkali and alkaline earth
233 metals, Fe, and a few other trace elements (the concentrations of these dissolved species did not
234 exceed national regulatory drinking water standards).

235 Zheng et al. [26] ran modeling analyses to interpret the groundwater quality response to CO_2
236 injection at the MSU-ZERT site. It was determined that a dynamic reactive-transport model could
237 not be well constrained because only a short period of the test was unaffected by rainfall, and fast,
238 gaseous CO_2 migration in the vadose zone appeared to have contributed to the groundwater
239 response to CO_2 injection. For these reasons, geochemical modeling analyses were conducted
240 instead, examining groundwater chemistry as a function of pH and P_{CO2}, independently of time.
241 The geochemical modeling analyses were supplemented with principal component (statistical)
242 analyses of the groundwater chemistry data, which suggested a correlated response to carbonation
243 for alkali and alkaline earth metals, and another different correlated response for trace metals
244 forming oxyanions (e.g., As, Se). Based on these investigations, Zheng et al. [26] suggested that at
245 this site, groundwater carbonation drove calcite dissolution, which resulted in the release of Ca,
246 which in turn drove exchange reactions with most major and trace metal cations. The release of Fe
247 was attributed to the dissolution of reactive Fe minerals (presumably ferrihydrite and/or fougerite
248 "green rust"), and the release of anions (As, Se) to competitive adsorption of carbonate. Both field
249 data[17] and modeling results[26] showed a progressive increase in metal concentrations with a pH
250 decrease (and alkalinity increase), and a quick return to background concentrations after the
251 injection stopped.

252 The longer test period and extensive data set collected during the Mississippi field
253 experiment[19] allowed for the development of 1D, 2D, and 3D reactive transport models of this
254 field experiment, drawing on extensive hydrogeologic and geochemical characterization efforts,
255 including detailed investigations of mineral-sediment associations by wet chemistry methods,

256 spectroscopic analyses, and laboratory CO_2 leaching experiments.[9,19] A horizontal 2D reactive
257 transport model was presented in Trautz et al.[19]

258 At the Mississippi site, the pH drop (by ~3 units) upon carbonation was initially accompanied
259 by a pulse-like increase in the concentration of major cations (Ca, Na, Mg, K) and some trace
260 metals (e.g., Ba, Fe, Sr, Mn) (Figure 1). Initial reactive transport simulations[19] showed that this
261 behavior could be reproduced by processes similar to those postulated for the MSU-ZERT site,
262 namely Ca from calcite dissolution driving exchange reactions with alkali and alkaline earth
263 metals, and dissolution of Fe sulfides releasing Fe. However, one important difference between
264 these test sites is the abundance of calcite at the MSU-ZERT site, compared to the rare occurrence
265 of this mineral at the Mississippi site, where it was found only in minute quantities, well below
266 conventional XRD and TIC-TOC detection limits. Our previous modeling analyses[19] showed that
267 fast and complete dissolution of a limited amount of calcite could explain the observed pulse-like
268 behavior of dissolved Ca concentrations, and of other cations by exchange with Ca (Figure 1).
269 Modeling also showed that fast desorption could be an alternative process, yielding pulse-like
270 concentration trends for Ca, Fe, and other cations.

271 After publication of our initial results[19], post-injection monitoring at the Mississippi site
272 revealed that the pulse-like response of dissolved metals observed during injection was followed
273 by slow-rising concentrations of alkali and alkaline earth metals starting almost immediately after
274 the end of the injection period (Figure 2). Also, the pH remained depressed at all monitoring wells
275 after the pump was turned off. This finding is different from observations at the MSU-ZERT site,
276 where the groundwater composition and pH quickly returned to ambient background conditions
277 after the injection of CO_2 was stopped.[17] The contrasting behavior at these two sites may be
278 explained by the differences in regional hydraulic gradient and pH buffering capacity at these
279 sites. The abundance of carbonate minerals (buffering pH) and steep hydraulic gradient at the
280 MSU-ZERT site are favorable conditions for a quick pH rebound and fast return to background

concentrations of dissolved species after CO_2 injection. In contrast, the hydraulic gradient at the Mississippi site is small, and sediments have a low buffering capacity. Thus, it is suggested that once injection ended, the return to slow groundwater velocities (thus increasing residence time) and persisting low pH provided conditions favoring continued (and increased) reactions between sediments and groundwater.

To test this hypothesis, further modeling analyses were performed as part of the present study. Simple reactive transport models were constructed using the same setup and mineralogical, thermodynamic and kinetic data as implemented in our initial investigations[19] (Appendix A). In these new simulations, sediment-bound metals were included in the form of both (a) a fast-reacting but limited pool, yielding a pulse-like response to a pH drop (as in initial simulations[19]) but also (b) a slow-reacting but essentially unlimited pool, yielding rising dissolved metal concentrations only upon decreased groundwater velocities, after the injection was ended. Such conceptualization combines the initial fast pulsing behavior reported earlier[19], together with transport-limited kinetic dissolution trends (e.g., Johnson et al.[28]) that are strongly dependent on groundwater residence times, and only noticeable when the groundwater velocity is slow relative to reaction rates or inversely, when reaction rates are fast relative to the groundwater velocity.

In the present study we applied this concept to the Mississippi test experiment, by modeling the fast dissolution of a limited amount of calcite, superimposed with the slow dissolution of plagioclase (ubiquitous in the sediments). Four simulations were run: a base-case that considers the fast-reacting Ca pool (calcite) but no slow-reacting pool (no plagioclase, as in our previous model[19]) and three other cases with the addition of plagioclase dissolution, at a different rate for each case. Results show (Figure 2) that when the slow dissolution of plagioclase is added in the simulations, both the observed short- and long-term concentration trends of Ca can be reproduced fairly well (Figure 2), with the slow rise in Ca concentration becoming noticeable only during the post-injection period when groundwater velocities returned to small values (essentially stagnant

hydraulic gradient < 0.0001 in this case). By Ca-driven cation exchange, the observed parallel trend of Ba concentrations (and other cations as well) is also well reproduced (Figure 2).

These simulations convey the importance of considering groundwater residence time when interpreting the results of field experiments and/or assessing the potential impact of CO_2 release at a particular site. The slow dissolution of minerals (by carbonic acid from CO_2 dissolution) is likely to present more of a potential concern (and be more noticeable) at sites where the regional groundwater flow rate is low. Also, the fact that most laboratory experiments to investigate CO_2 impacts on groundwater are conducted under "batch" (stagnant) conditions may explain why the release of metals observed in these experiments is generally much more noticeable than in the field, where groundwater is seldom stagnant.

4. Modeling Interpretation of Laboratory Experiments

We report here on the modeling of sequential leaching tests[9] conducted on two sandy sediment samples collected from the injection interval at the Mississippi field site[19] (these sequential leaching tests were conducted to supplement the field test and evaluate possible screening procedures[9]). The goal of this modeling effort was to determine whether the same geochemical processes simulated to reproduce the field test results could also explain the results of these laboratory experiments. To set the stage for this modeling investigation, before discussing its results, we first summarize below the experimental procedure followed by Varadharajan et al.[9] (readers are referred to their paper for more details).

4.1 Summary of experimental approach

In the experiments carried out by Varadharajan et al.[9], synthetic groundwater solutions were initially brought into contact with sandy sediments that were air-dried in a glove box. The solutions were allowed to equilibrate with the sediments, then subsequently sampled and replaced with fresh groundwater at time intervals of 1, 4, 11, and 25 days after the start of each experiment.

Two different types of experiments were used to distinguish between pH-driven and carbonate-driven metal-release reactions. The first setup involved pressurized reactor cells (at pressure ~ 4 bar) that were filled with synthetic groundwater solutions saturated with CO_2, hereafter referred to as the "CO_2-saturated" system. The second setup used vials that were filled with pH-amended, synthetic groundwater solutions equilibrated with a CO_2-free atmosphere at atmospheric pressure, and acidified with HCl to evaluate metal release driven by pH effects alone. These experiments are hereafter referred to as the "pH-amended" system. The solid:solution ratio was maintained at 1:4.5 in the "CO_2-saturated" case, and 1:4 in the "pH-amended" case. Synthetic groundwater was prepared with a composition similar to groundwater at the Mississippi field site, 6.4 mM $NaHCO_3$, 0.7 mM NaCl, 0.1 mM KCl, 0.1 mM CaCl2, and 0.3 mM Na-acetate; no trace elements were added to the solution.

4.2 Modeling Approach and Results

The numerical model was designed to mimic experimental procedure as closely as possible. The water-sediment system was modeled as a "batch" system with a total volume of 1 L. The solution (synthetic groundwater) was numerically reacted with the sediments and subsequently withdrawn and replenished with fresh solution at the prescribed periods of time (1, 4, 11, and 25 days) to match the experimental procedure. The same synthetic groundwater composition and solid-to-solution ratios were assumed as in the actual experiments. The chemical reactions and reactive processes considered in the model were the same as those used for modeling the Mississippi field test (Appendix A).

The same geochemical conceptual model, as adopted to simulate the MSU-ZERT and Mississippi field tests (as presented earlier) was used to model the laboratory experiments; it is thus postulated that the drop in pH induces the dissolution of calcite, and that the resulting increase in Ca concentration subsequently triggers a series of cation exchange reactions, leading to an

increase in the concentrations of alkaline earth cations. The values of two key model input parameters, the volume fraction of calcite and its specific surface area, were modified from the values adopted to model the field test in order to match the experimental data. The volume fraction of calcite was changed from 0.0086% (calibrated after the field test data) to 0.0073% in the "CO_2-saturated' case, and 0.0096% for the "pH-amended" case (calibrated after the laboratory test data), which are essentially insignificant changes that could easily be attributed to heterogeneity or measurement uncertainty. However, the dissolution of calcite had to be accelerated by increasing the calcite specific surface area by two orders of magnitude (Equation A–1). Such an increase is within the range typical of the discrepancy observed between field- and laboratory-scale rates (e.g., Zhu,[29]). For example, Yang et al.[16] also mentioned that reaction rates estimated from batch experiments using sediments from their test site were generally higher than those observed in the field push-pull test. The use of a larger calcite surface area when modeling the laboratory experiments can also be justified by the fact that the unconsolidated sediments in the reactor cells were well-stirred to ensure good mixing and maximize the surface area available for reactions. Figures 3 and 4 show the sensitivity of calculated Ca and Sr concentrations to the volume fraction and specific surface area of calcite, indicating the need to change both the volume fraction of calcite and its specific surface area to match the measured Ca and Sr concentrations.

An alternative conceptual model proposed by other studies[4,10,11] is based on impurities that may be present in carbonate minerals being the source of metals released when sediments are reacted with carbonated water. To test this concept, we removed Sr from the list of exchangeable cations, and instead included 1.5 mol% Sr impurity to calcite, an amount that was calibrated to match the experimental results (in doing so, we also recomputed the equilibrium constant for Sr-calcite by assuming an ideal solid solution between calcite and strontianite.) Figure 5 shows that calcite with 1.5% Sr impurity leads to a reasonably good fit of the measured data, although the

concept of calcite dissolution plus cation exchange[26] adopted in the aforementioned models seems to perform slightly better in terms of capturing the temporal changes. Nevertheless, considering the large uncertainties exhibited by the data, this modeling exercise is unable to distinguish which concept is more plausible.

5. The Question of Reversibility

It is well known that the exsolution of CO_2 from groundwater increases the water pH (reverse of reactions 1 and 2) and thus is likely to result in immobilization metals by reversing Reactions 3 to 8. Examples of mineral precipitation upon CO_2 exsolution include the treatment of ferruginous groundwater by pressure-driven CO_2 degassing[30], and the observation of dolomite precipitation upon CO_2 exsolution (in this case thermally driven exsolution) during a CO_2-dolomite reaction experiment.[31] In fact, some metallic ore deposits are known to have formed due to the pH rise driven by exsolution of CO_2 (and other acid gases) upon depressurization and boiling when metal-loaded thermal waters ascend to the surface[32]. Furthermore, many naturally carbonated mineral spring waters are of excellent (drinking) quality with respect to priority pollutant metal concentrations.[33] Therefore, a logical question to raise is whether the mobilization of metals at depth, by CO_2-saturated water could be mitigated when groundwater ascends toward the surface and progressively depressurizes, leading to CO_2 exsolution.

To help illustrate this process in the context of shallow groundwater aquifers, we conducted numerical experiments using simple geochemical simulations (Appendix B). In the first stage, the CO_2-driven (P_{CO2} ~ 5 bar) dissolution of FeS and trace-metal-bearing (Ba, Pb, Ni) calcite was simulated, accompanied by desorption of cations (Fe^{+2}, Ni^{+2}, Ba^{+2}, and Pb^{+2}) from a sorbent arbitrarily modeled as iron hydroxide (ferrihydrite). In a second stage, the depressurization of this system was simulated down to atmospheric P_{CO2} levels, leading to re-sorption and re-precipitation of trace metal-bearing calcite and also siderite. The degassing stage was conducted with water in contact with the minerals and sorbent considered (i.e., solution with sediments), and then repeated

without contact with minerals or sorbent (i.e., with sediments removed from the solution). The same initial general geochemical conditions as observed at the Mississippi field test site were assumed, including the input water composition reported by Trautz et al.[19], yielding a pH drop from ~8 to ~5.6 upon CO_2 pressurization (Figure 6). However, it should be emphasized that these simulations were not intended as predictions of the Mississippi field test, and are only meant to illustrate the effect of CO_2 degassing in a generic, mostly qualitative manner.

Results are examined independently of time by plotting pH and aqueous metal concentrations as a function of CO_2 pressure for the cases considered (Figure 7). Upon degassing of CO_2, the concentrations of metals and pH return close to their original values, except for Ni in the case without sediments. This is because in this example, the behavior of Ni is dominated by sorption/desorption, whereas the concentrations of the other metals are mostly controlled by dissolution/precipitation. Removing the sediment in this case obviously prevents Ni from re-sorbing upon CO_2 degassing. In contrast, the concentration of Fe upon pressurization with CO_2 is controlled by the dissolution of FeS followed by siderite precipitation, which is not initially present but allowed to form. The concentrations of other metals (including Pb on Figure 7) are dominated by the dissolution and re-precipitation of metal-bearing calcite, assuming reversibility in the partitioning of trace elements, for simplicity. Upon degassing, without sediments present, there is no precursor surface area for precipitation, which allows for a certain amount of supersaturation to be reached until precipitation occurs (through a scheme approximating nucleation implemented into the TOUGHREACT code[35]). This causes a discontinuous pH curve and unsymmetrical behavior between the CO_2 dissolution and exsolution stages (Figure 7), but as would be expected, all paths for metals controlled by precipitation/dissolution eventually return close to their starting points. These somewhat simplistic simulations illustrate how the system behavior upon depressurization depends on the differences between dissolution and precipitation rates (which in turn depend partially on differences in surface areas available for dissolution and

precipitation), relative rates of carbonate mineral precipitation (e.g., calcite vs. siderite), and on whether sorption is considered reversible or not. Concentration trends also depend on the partitioning (solid-solution) behavior of trace elements into re-precipitated carbonates, as a function of water chemistry. All these characteristics are expected to be strongly influenced by the physical path taken by groundwater as it ascends toward the surface. Therefore, the overall risk of potential CO_2 leakage into groundwater should not only consider the chemical impact of carbonic acid on the mobilization of metals, but should also take into account the path of contaminated groundwater to potential receptors at shallow depths where the ambient pressure is too low to maintain elevated CO_2 (carbonic acid) concentrations into solution.

6. Summary and Conclusion

The controlled release of CO_2 into shallow aquifers at the MSU-ZERT and Mississippi test sites provided a unique opportunity to combine numerical modeling analyses with extensive datasets collected in the field and the laboratory, to assess the effects of potential CO_2 leaks from deep storage formations on the quality of freshwater aquifers. At both sites, the groundwater pH responded quickly to carbonation, dropping by about 0.8 pH units in the MSU-ZERT experiment (a well-buffered system) and about 3 pH units in the Mississippi experiment (a poorly buffered system). At both sites, the pH decrease was accompanied primarily by increased dissolved concentrations of alkali and alkaline earth metals as well as Fe. The concentrations of a few other trace metals also increased, but to a lesser extent, and never exceeding regulatory limits. The main differences in response to carbonation at these sites were the types of concentration profiles observed with time for mobilized constituents. Fairly continuous increases with time (and pH drop) were observed at the MSU-ZERT site, followed by a quick return to background conditions once carbonation ended[17]. At the Mississippi site, however, the carbonation of groundwater first yielded a pulse of mobilized constituents[19], followed by slow concentration increases after the

457 injection ended (when the groundwater flow velocity decreased). The slow rise in concentrations
458 eventually reached new plateaus although the pH remained depressed for months after the
459 injection ended. This contrasting behavior at these two test sites is attributed to the slow ambient
460 groundwater velocity and lower pH buffering capacity (very small amounts of carbonate minerals)
461 at the Mississippi site compared to the MSU-ZERT site.

462 Characterization and modeling studies of the field data suggest that at both sites, calcite
463 dissolution, ion exchange and/or desorption were the primary mechanisms of initial (fast) release
464 of alkali and alkaline earth metals. Effects from slow dissolution of other minerals were only
465 noticeable in the Mississippi field experiment after the injection ended, due to the slow ambient
466 groundwater velocity at this site once the pump was turned off. This shows that the ambient
467 groundwater flow rate is an important parameter to consider, in addition to the pH buffering
468 capacity of an aquifer, when evaluating the potential impact of CO_2 leakage on groundwater
469 quality.

470 A series of previously published laboratory sequential leaching tests[9] using sediments from the
471 Mississippi site were simulated. By applying our conceptual model of Ca-driven cation exchange
472 previously developed for the MSU-ZERT field test[26], then cross-tested with simulations of the
473 Mississippi field experiment[19], we were able to simulate these laboratory experiments reasonably
474 well, and explain differences observed between laboratory and field test results. Our simulations
475 suggest that calcite dissolution and Ca-driven cation exchange may control the initial release of
476 alkali and alkaline earth metals in both the field and laboratory experiments, although the
477 dissolution of calcite containing metal impurities cannot be ruled out as another potential
478 mechanism of metal release.

479 A higher dissolution rate of calcite, compared to the rate used to model the field experiments,
480 was required to model the laboratory data. This suggests that laboratory tests might be too
481 aggressive in leaching out trace elements, relative to what would be expected in the field, as

482 solution and sediment are well mixed under a no-flow condition in the laboratory tests. This
483 should be taken into account when laboratory tests are used to evaluate the potential impact of
484 CO_2 leakage on groundwater quality.

485 Simple, generic numerical experiments illustrated how the mobilization of metals under
486 elevated P_{CO2} could be reversed under depressurization, which would occur when groundwater
487 ascends (or is pumped) to the ground surface and CO_2 volatilizes under decreasing hydrostatic
488 pressure. The extent of reversibility is likely to depend on the path followed by groundwater when
489 it is brought to the surface, both in terms of physical path (affecting the surface area available for
490 metal re-precipitation and/or re-sorption) and temperature-pressure path (affecting the
491 thermodynamic drive for these reactive processes). The largest reversal would be expected to
492 occur between P_{CO2} of a few bar and atmospheric values, when the gradient of pH change with
493 P_{CO2} is the steepest. In contrast, the potential impacts from the mobilization of organic
494 compounds[25] and brine displacement[34] by supercritical CO_2 in deep saline aquifers, followed by
495 leakage to shallow groundwater bodies, could be much less reversible, and therefore may warrant
496 more attention than the impact from the CO_2 alone. However, the sequestration of metals by
497 resorption and re-precipitation upon CO_2 exsolution, in the context of impacts from CO_2 leakage,
498 has been given little attention and may warrant more study investigating the effects of CO_2
499 pressurization and depressurization along different flow paths.

500 Reactive transport models are important tools being used to assess the potential risk of CO_2
501 geological sequestration to groundwater over long periods of time. Geochemical reaction networks
502 implemented in these simulations form the core of such models. This paper demonstrates that the
503 close integration of field and laboratory tests with numerical modeling is crucial to assess various
504 key geochemical reactions and parameters, and thus to increase the confidence in, and
505 predictability of, numerical models.

506

ACKNOWLEDGMENT

This work was supported by the Electric Power Research Institute; the EPA, Office of Water, under an Interagency Agreement with the U.S. Department of Energy (DOE) at LBNL, under contract number DE-AC02-05CH11231; and the Assistant Secretary for Fossil Energy, National Energy Technology Laboratory (NETL), National Risk Assessment Program (NRAP), of the US Department of Energy under Contract No. DEAC02-05CH11231.

References

1. Lemieux J-M. Review: The potential impact of underground geological storage of carbon dioxide in deep saline aquifers on shallow groundwater resources. *Hydrogeology Journal* 19(4): 757-778 (2011).
2. Harvey OR, Qafoku NP, Cantrell KJ, Lee G, Amonette JE, Brown CF. Geochemical Implications of Gas Leakage associated with Geologic CO_2 Storage—A Qualitative Review. *Environmental Science & Technology* 47(1): 23-36 (2012).
3. Smyth RC, Hovorka SD, Lu J, Romanak KD, Partin JW, Wong C, et al. Assessing risk to fresh water resources from long term CO_2 injection-laboratory and field studies. *Energy Procedia* 1(1): 1957-1964 (2009).
4. Lu JM, Partin JW, Hovorka SD, Wong C. Potential risks to freshwater resources as a result of leakage from CO_2 geological storage: a batch-reaction experiment. *Environmental Earth Sciences* 60(2): 335-348 (2010).
5. Little MG, Jackson RB. Potential Impacts of Leakage from Deep CO_2 Geosequestration on Overlying Freshwater Aquifers. *Environmental Science & Technology* 44(23): 9225-9232 (2010).

6. Wei Y, Maroto-Valer M, Steven MD. Environmental consequences of potential leaks of CO_2 in soil. *Energy Procedia* 4(0): 3224-3230 (2011).
7. Viswanathan H, Dai Z, Lopano C, Keating E, Hakala JA, Scheckel KG, et al. Developing a robust geochemical and reactive transport model to evaluate possible sources of arsenic at the CO_2 sequestration natural analog site in Chimayo, New Mexico. *International Journal of Greenhouse Gas Control* 10(0): 199-214 (2012).
8. Humez P, Lagneau V, Lions J, Negrel P. Assessing the potential consequences of CO_2 leakage to freshwater resources: A batch-reaction experiment towards an isotopic tracing tool. *Applied Geochemistry* 30(0): 178-190 (2013).
9. Varadharajan C, Tinnacher RM, Pugh JD, Trautz RC, Zheng L, Spycher NF, et al. A laboratory study of the initial effects of dissolved carbon dioxide (CO_2) on metal release from shallow sediments. *International Journal of Greenhouse Gas Control* 19(0): 183-211 (2013).
10. Wunsch A, Navarre-Sitchler AK, Moore J, McCray JE. Metal release from limestones at high partial-pressures of CO_2. *Chemical Geology* 363(0): 40-55 (2014).
11. Kirsch K, Navarre-Sitchler AK, Wunsch A, McCray JE. Metal Release from Sandstones under Experimentally and Numerically Simulated CO_2 Leakage Conditions. *Environmental Science & Technology* 48(3): 1436-1442 (2014).
12. Keating EH, Fessenden J, Kanjorski N, Koning DJ, Pawar R. The impact of CO_2 on shallow groundwater chemistry: observations at a natural analog site and implications for carbon sequestration. *Environmental Earth Sciences* 60(3): 521-536 (2010).
13. Peter A, Lamert H, Beyer M, Hornbruch G, Heinrich B, Schulz A, et al. Investigation of the geochemical impact of CO_2 on shallow groundwater: design and implementation of a CO_2 injection test in Northeast Germany. *Environmental Earth Sciences* 67(2): 335-349 (2012).

14. Cahill AG, Jakobsen R. Hydro-geochemical impact of CO_2 leakage from geological storage on shallow potable aquifers: A field scale pilot experiment. *International Journal of Greenhouse Gas Control* 19(0): 678-88 (2013).
15. Gal F, Prousta E, Humeza P, Braibanta G, Bracha M, Kocha F, Widory D, Girarda JF. Inducing a CO_2 leak into a shallow aquifer (CO_2FieldLab EUROGIA+ project): Monitoring the CO_2 plume in groundwaters. GHGT-11 proceedings paper. Energy Procedia 37, 3583–3593 (2013).
16. Yang C, Mickler PJ, Reedy R, Scanlon BR, Romanak KD, Nicot J-P, et al. Single-well push–pull test for assessing potential impacts of CO_2 leakage on groundwater quality in a shallow Gulf Coast aquifer in Cranfield, Mississippi. *International Journal of Greenhouse Gas Control* 18(0): 375-87 (2013).
17. Kharaka YK, Thordsen JJ, Kakouros E, Ambats G, Herkelrath WN, Beers SR, et al. Changes in the chemistry of shallow groundwater related to the 2008 injection of CO2 at the ZERT field site, Bozeman, Montana. *Environmental Earth Sciences* 60(2): 273-84 (2010).
18. Spangler LH, Dobeck LM, Repasky KS, Nehrir AR, Humphries SD, Barr JL, et al. A shallow subsurface controlled release facility in Bozeman, Montana, USA, for testing near surface CO2 detection techniques and transport models. *Environmental Earth Sciences* 60(2): 227-39 (2010).
19. Trautz RC, Pugh JD, Varadharajan C, Zheng L, Bianchi M, Nico PS, et al. Effect of Dissolved CO_2 on a Shallow Groundwater System: A Controlled Release Field Experiment. *Environmental Science & Technology* 47(1): 298-305 (2013).
20. Wang S, Jaffe PR. Dissolution of a mineral phase in potable aquifers due to CO_2 releases from deep formations; effect of dissolution kinetics. *Energy Conversion and Management* 45: 2833-2848 (2004).

21. Carroll S, Hao Y, Aines R. Geochemical detection of carbon dioxide in dilute aquifers. *Geochemical Transactions* 10(4): 1-18 (2009).
22. Zheng L, Apps JA, Zhang Y, Xu T, Birkholzer JT. On mobilization of lead and arsenic in groundwater in response to CO_2 leakage from deep geological storage. *Chemical geology* 268(3-4): 281-297 (2009).
23. Apps JA, Zheng L, Zhang Y, Xu T, Birkholzer JT. Evaluation of groundwater quality changes in response to CO_2 leakage from deep geological storage. *Transport in Porous Media* 82(1): 215-246 (2010).
24. Wilkin RT, Digiulio DC. Geochemical Impacts to Groundwater from Geologic Carbon Sequestration: Controls on pH and Inorganic Carbon Concentrations from Reaction Path and Kinetic Modeling. *Environmental Science & Technology* 44(12): 4821-4817 (2010).
25. Zheng L, Spycher N, Birkholzer J, Xu T, Apps J, Kharaka Y. On modeling the potential impacts of CO_2 sequestration on shallow groundwater: Transport of organics and co-injected H_2S by supercritical CO_2 to shallow aquifers. *International Journal of Greenhouse Gas Control* 14(0): 113-27 (2013).
26. Zheng L, Apps JA, Spycher N, Birkholzer JT, Kharaka YK, Thordsen J, et al. Geochemical modeling of changes in shallow groundwater chemistry observed during the MSU-ZERT CO_2 injection experiment. *International Journal of Greenhouse Gas Control* 7(0): 202-17 (2012).
27. Kharaka YK, Thordsen JJ, Hovorka SD, Nance S, Cole DR, Phelps TJ, et al. Potential environmental issues of CO_2 storage in deep saline aquifers: Geochemical results from the Frio-I Brine Pilot test, Texas, USA. *Applied Geochemistry* 24: 1106-12 (2009).

28. Johnson JW, Knauss KG, Glassley WE, DeLoach LD, Tompson AFB (1998) Reactive transport modeling of plug-flow reactor experiments: quartz and tuff dissolution at 240°C. Journal of Hydrology, 209 (1–4), 81−111.
29. Zhu C. In situ feldspar dissolution rates in an aquifer. *Geochimica et Cosmochimica Acta* 69(6): 1435-53 (2005).
30. Geroni JN, Cravotta CA, Sapsford DJ. Evolution of the chemistry of Fe bearing waters during CO_2 degassing. Applied Geochemistry 27, 2335–2347 (2012) .
31. Tutolo BM, Luhmann AJ, Kong XZ, Saar MO, Seyfried WE (2014) Experimental observation of permeability changes in dolomite at CO_2 sequestration conditions. *Environ. Sci. Technol.* 48, 2445−2452 (2014).
32. Drummond SE and Ohmoto H. Chemical evolution and mineral deposition in boiling hydrothermal systems. *Economic Geology* 80: 1427-1439 (1985).
33. Allen HE, Halley-Henderson M, Hass CN Chemical composition of bottled mineral water. *Archives of Environmental Health: An International Journal* 44(2): 102-116 (1989).
34. Birkholzer JT, Zhou Q, Tsang C-F. Large-scale impact of CO_2 storage in deep saline aquifers: A sensitivity study on pressure response in stratified systems. *International Journal of Greenhouse Gas Control* 3: 181-94 (2009).
35. Xu T, Spycher N, Sonnenthal E, Zhang G, Zheng L, Pruess K. TOUGHREACT Version 2.0: A simulator for subsurface reactive transport under non-isothermal multiphase flow conditions. *Computers & Geosciences* 37(6): 763-74 (2011).
36. Lasaga AC, Soler JM, Ganor J, Burch TE, Nagy KL. Chemical weathering rate laws and global geochemical cycles. *Geochimica et Cosmochimica Acta* 58: 2361-8 (1994).
37. Plummer LN, Parkhurst DL, Wigley TML. Critical review of the kinetics of calcite dissolution and precipitation, in Chemical Modeling in aqueous System, Jenne E.; ACS Symposium Series; Ameridan Chemical Society: Washington, DC. (1979).

628 38. Palandri J, Kharaka YK. A compilation of rate parameters of water-mineral interaction
629 kinetics for application to geochemical modeling: US Geol. Surv. Open File report 2004-
630 10682004.
631 39. Wolery T. and Jove-Colon C., 2007. *Qualification of Thermodynamic Data for*
632 *Geochemical Modeling of Mineral-Water Interactions in Dilute Systems.* ANL-WIS-GS-
633 000003 REV 01. Las Vegas, Nevada: Sandia National Laboratories. ACC:
634 DOC.20070619.0007.
635 40. Johnson JW, Oelkers E, Helgeson HC. SUPCRT92: A software package for calculating the
636 standard molal thermodynamic properties of minerals, gases, aqueous species and reactions
637 from 1 to 5000 bar and 0 to 1000°C. *Comput Geosci,* (18) 899–947 (1992)..
638 41. Shock E, Sassani D, Willis M, Sverjensky D, Inorganic species in geo-logic fluids:
639 correlations among standard molal thermodynamic properties of aqueous ions and
640 hydroxide complexes. *Geochim. Cosmochim. Acta* 61:907–950 (1997).
641 42. Helgeson HC, Delany JM, Nesbitt HW, Bird DK. Summary and Critique of the
642 Thermodynamic Properties of Rock Forming Minerals. American Journal of Science, 278-
643 A, (1978).
644 43. Appelo CJA, Postma D. Geochemistry, groundwater and pollution. Rotterdam,
645 Netherlands: A.A.Balkema,(1994).
646 44. Dzombak DA, Morel FMM. surface complexation modeling-hydrous ferric oxide. New
647 York: John wiley & sons, (1990).
648 45. Appelo CAJ, Van Der Weiden MJJ, Tournassat C, Charlet L. Surface complexation of
649 ferrous iron and carbonate on ferrihydrite and the mobilization of arsenic. *Environ Sci*
650 *Technol* 36(14): 3096-103 (2002).
651 46. Liger E, Charlet L, van Cappellen P. Surface catalysis of uranium(VI) reduction by
652 iron(II). *Geochimica et Cosmochimica Acta*, 63(19/20):2939–2955, (1999)

Appendix A – Mississippi Field Site Reactive-Transport-Model Mineralogical, Thermodynamic, and Kinetic Data

Modeled geochemical processes include aqueous complexation, surface complexation (using a double diffuse layer model), cation exchange (using the Gaines-Thomas convention), and mineral precipitation/dissolution under kinetic constraints (using published rate laws). The implemented cation exchange reactions and selectivity coefficients are listed in Table A-1. In this model, it is assumed that ferrihydrite (as $Fe(OH)_3(s)$), is the adsorbent, and the surface complexation reactions and constants are listed in Table A-2. Based on the sediment mineralogical characterization,[9] the model considered illite, smectite, $Fe(OH)_3(s)$ and amorphous iron sulfide (mackinawite, FeS(m)), in addition to major aquifer minerals such as quartz, K-feldspar, and plagioclase (Ab80An20). The amount of iron sulfide (FeS(m)) was estimated from selective extraction data (~0.02 vol%), and the amount of $Fe(OH)_3(s)$ from the sediment acid titration data (~0.015 vol%), assuming this phase dominates H^+ sorption, as a first approximation. Carbonates were not detected using XRD and solid TIC-TOC analysis, but very rare gains in calcite were found by micro-X ray spectroscopy. Therefore, trace amounts of calcite were included in the simulations (0.0058%), an amount that was calibrated to yield best match of observed and modeled Ca response to CO_2 release. The amount of illite, smectite, quartz, and K-feldspar were roughly estimated from examinations of sediment cores and thin sections.

The simulations are conducted with TOUGHREACT[35] which uses a general form of rate expression: [36]

$$r = kA\left|1 - \left(\frac{K}{Q}\right)^{\theta}\right|^{\eta} \quad \text{(A-1)}$$

where r is the kinetic rate, k is the rate constant (mol/m^2/s), which is temperature dependent, A is the specific reactive surface area per kg H_2O, K is the equilibrium constant for the mineral–water

reaction written for the destruction of one mole of mineral, and Q is the reaction quotient. Here, we set the parameters θ and η to unity. The rate constant for calcite dissolution is given as a combination of neutral, acid, and carbonate mechanisms: [37,38]

$$k = 1.5 \times 10^{-6} e^{-E_a^{nu}/RT} + 0.5 e^{-E_a^{H}/RT} \alpha_H + 9.6 \times 10^{-5} e^{-E_a^{CO2}/RT} \alpha_{CO2} \quad \text{(A-2)}$$

where E_a^{nu}, E_a^{H} and E_a^{CO2} are activation energies with values of 23.5, 14.4, and 35.4 (kJ/mol) respectively, according to Palandri and Kharaka.[38] 1.5×10^{-6}, 0.5 and 9.6×10^{-5} are rate constant in mol/m^2/s for neutral, acid, and carbonate mechanisms, respectively. α_H is the activity of proton and α_{CO2} is the activity of dissolved CO_2. R is the gas constant. The surface area, A, is a function of specific surface area and the abundance of minerals. The specific surface area of calcite was set to 9.8 cm^2/g, a value which was calibrated, together with the initial calcite volume fraction, to match the breakthrough curves of alkaline earth metals observed during the field experiment at the Mississippi site. It should be noted that reaction rates depend on the reactive surface area A in Equation A-1, which is a function of the product of the specific surface area and the volume fraction of each mineral. Therefore, the calibrated values of specific surface area and volume fraction of calcite should be viewed as arbitrary and non-unique (co-linearly varying) values, the product of which being of relevance but not each value separately.

Thermodynamic data (Table A-3) were taken primarily from the EQ3/6 database *data0.ymp.R4*, [39] which relies on Gibbs free energy data primarily from SUPCRT92[40,41] for aqueous species, and from Helgeson et al.[42] for minerals.

Appendix B – Setup of CO_2 reaction and degassing numerical experiments

The problem was run with TOUGHREACT V2[35] and the same thermodynamic database as used for the other simulations (Appendix A). CO_2 pressurization was simulated with one model gridblock, fully liquid-saturated, in contact with a 5-bar CO_2 gas buffer allowed to dissolve at a rate prescribed to yield stable pH values near ~5.5 within a couple months (down from ~8

706 initially) (Figure 6). The system at low pH and ~5 bar CO_2 was then allowed to degas through a
707 second large (essentially open) model gridblock at atmospheric CO_2 pressure, into which gas from
708 the first gridblock was allowed to slowly flow until atmospheric CO_2 levels was reached. The
709 leakage rate was adjusted such that the system returned to initial atmospheric CO_2 levels within
710 about 180 days (an arbitrary but realistic value).

711 Ba, Pb, and Ni were included in trace quantities into calcite (in arbitrary amounts of 2×10^{-5}
712 moles Ba, 0.5×10^{-5} moles Pb, and 0.5×10^{-5} moles Ni for each mole of Ca). These elements and Fe,
713 Ca, Mg, were also considered initially sorbed onto the sediment, assuming sorption data for iron
714 hydroxides from Dzomback and Morel,[44] except Fe^{+2} from Liger et al.[46] (from the *phreeqc.dat*
715 database, corrected for consistency with the other data). The solid phase (sediments) prior to
716 addition of CO_2 was assumed to contain (by solid volume) 10% plagioclase (An20), 0.1% FeS,
717 0.1% calcite, and 0.01% iron hydroxides (as ferrihydrite). Siderite was allowed to precipitate but
718 not assumed initially present. The initial water composition was taken from Trautz et al.[19], with
719 adjusted initial Fe, Ca, and Al concentrations to yield chemical equilibrium with FeS, calcite, and
720 pagioclase, respectively, at 25°C.
721

722 Table A-1. Cation exchange reactions and selectivity coefficients.[43]

Cation exchange reaction	$K_{Na/M}$
$Na^+ + X\text{-}H = X\text{-}Na + H^+$	1
$Na^+ + X\text{-}K = X\text{-}Na + K^+$	0.2
$Na^+ + 0.5X\text{-}Ca = X\text{-}Na + 0.5Ca^{+2}$	0.4
$Na^+ + 0.5X\text{-}Mg = X\text{-}Na + 0.5Mg^{+2}$	0.45
$Na^+ + 0.5X\text{-}Ba = X\text{-}Na + 0.5Ba^{+2}$	0.35
$Na^+ + 0.5X\text{-}Mn = X\text{-}Na + 0.5Mn^{+2}$	0.55
$Na^+ + 0.5X\text{-}Sr = X\text{-}Na + 0.5Sr^{+2}$	0.35
$Na^+ + 0.5X\text{-}Zn = X\text{-}Na + 0.5Zn^{+2}$	0.4
$Na^+ + X\text{-}Li = X\text{-}Li + Li^+$	1.1

723

724 Table A-2. Surface complexation reactions and surface complexation constants (logK) on
725 ferrihydrite. The reaction constants for surface protonation are from Dzombak and Morel[44] and
726 surface complexation reactions of carbonate are from Appelo et al.[45]

Surface complexation	logK
$HFO\_sOH_2^+ = HFO\_sOH + H^+$	-7.29
$HFO\_wOH_2^+ = HFO\_wOH + H^+$	-7.29
$HFO\_sO^- + H^+ = HFO\_sOH$	8.93
$HFO\_wO^- + H^+ = HFO\_wOH$	8.93
$HFO\_wCO_2^- + H_2O = HFO\_sOH + HCO_3^-$	-2.45
$HFO\_wCO_2H + H_2O = HFO\_sOH + HCO_3^- + H^+$	-10.4

727

728

729 Table A-3. Equilibrium constants and volume fraction for minerals

Primary Mineral	Volume fraction (%)	logK(25°C)	Secondary Mineral	logK(25°C)
Quartz	92	-3.75	Gypsum	-4.48
Calcite	0.0058*	1.85	Dolomite	2.52
FeS(m)	0.02	-3.5	Siderite	-0.25
K-feldspar	2	-22.39	Witherite	1.77
Smectite-Na	0.5	-38.32	Rhodochrosite	0.252
Illite	1	-42.69	Strontianite	-0.31
$Fe(OH)_3(s)$	0.15	-5.66	Dawsonite	-17.9
Ab80An20	4	-14.8		

730 *varies depending models

731

732

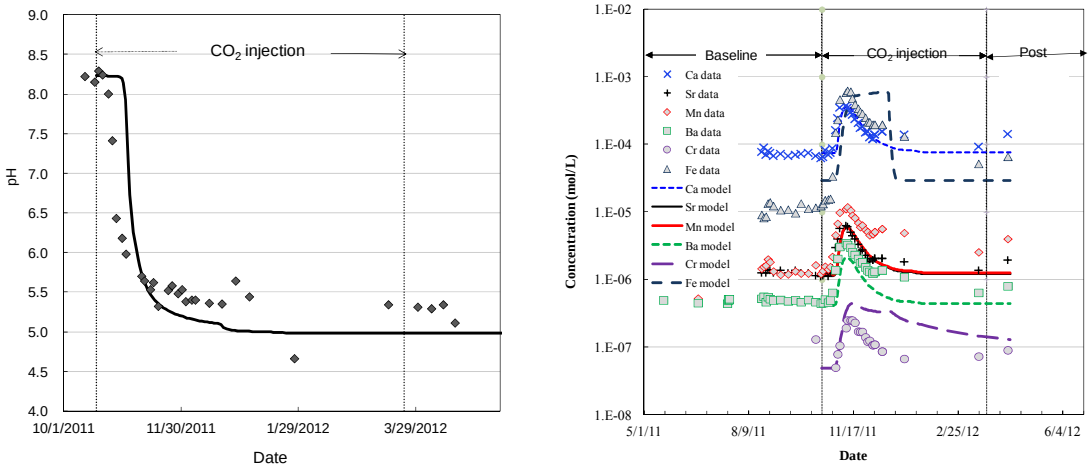

Figure 1. pH (left) and breakthrough of Ca, Sr, Mn, Ba, Cr, and Fe at about 5 m from a carbonated groundwater injection well; model predictions (lines) compared to observations (symbols) (data reported in Trautz et al. [19]).

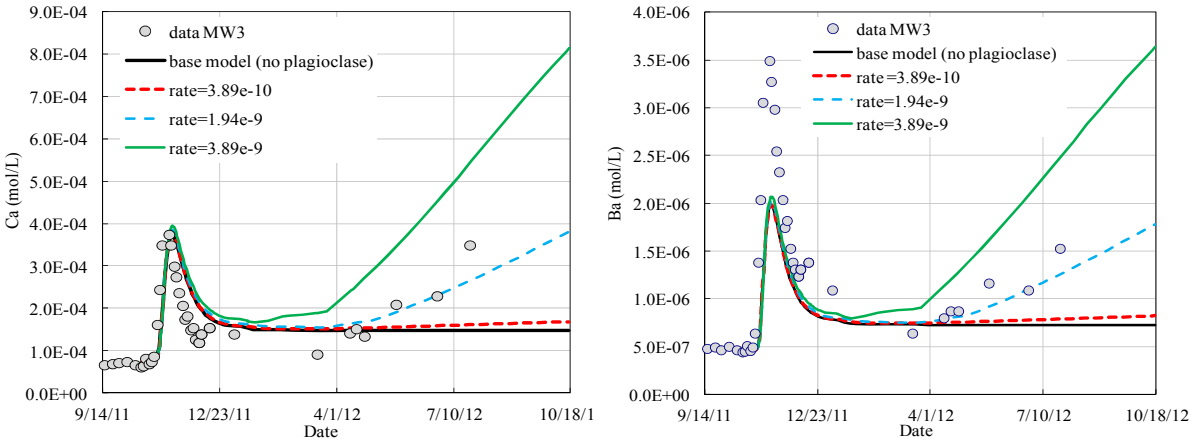

Figure 2. Observed (symbols) and modeled concentration time profiles (lines) for Ca on the left and Ba on the right. Model results are shown for a base-case considering only the presence of fast-dissolving calcite in a limited amount, and three other cases with added slow dissolution of plagioclase at different rates as shown (mol s^{-1} kg_w^{-1}). See text.

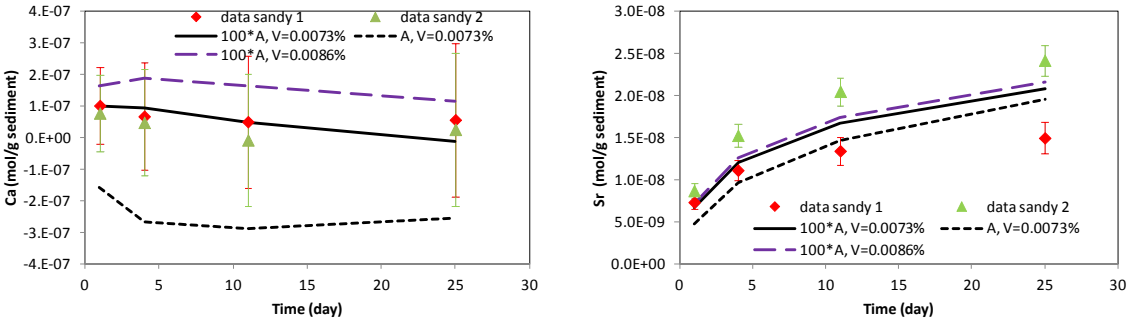

745

746 **Figure 3.** Measured Ca and Sr concentration (symbols) for the "pH-amended" experiment, and
747 model results (lines) using different combination of parameters (calcite volume fraction, V;
748 specific surface area, A; and the latter increased a hundred-fold, 100*A). Solute concentrations
749 represent net changes after the subtraction of respective background concentrations measured in
750 sediment-free controls, and normalized for solid weights (negative values represent uptake by the
751 sediments). All concentration values are averages of duplicate samples; error bars for the
752 laboratory data represent propagated standard errors based on analytical standard deviations and
753 duplicate samples.

754

755

756

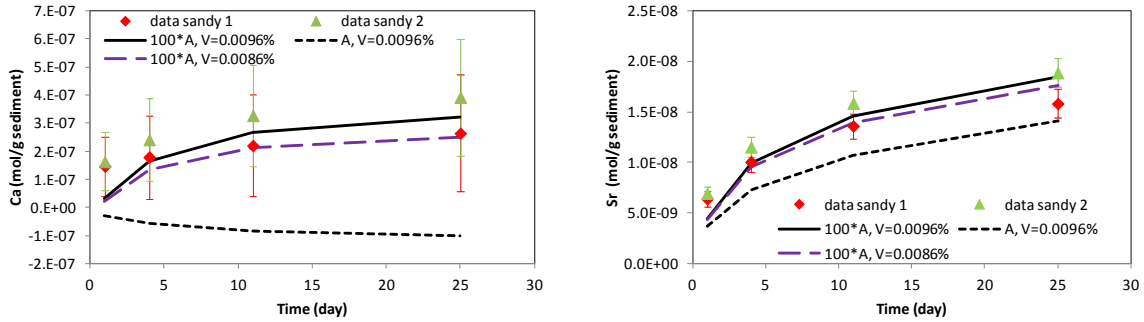

757

758 **Figure 4.** Measured Ca and Sr concentrations (symbols) for the "CO_2-saturated" experiment and
759 models results (lines) using different combinations of parameters. See caption of Figure 3 for
760 additional information.

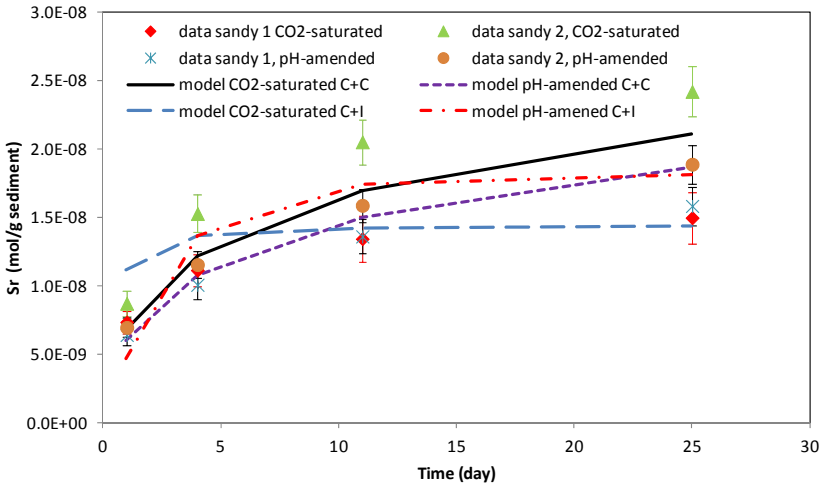

761

762 **Figure 5.** Measured Sr concentration (symbols) for "CO_2-saturated" and "pH-amended"
763 experiment and the corresponding simulated concentration (lines) using different conceptual
764 models: pure calcite dissolution plus cation exchange[26] (C+C) and dissolution of Sr-bearing calcite
765 (C+I).

766

767

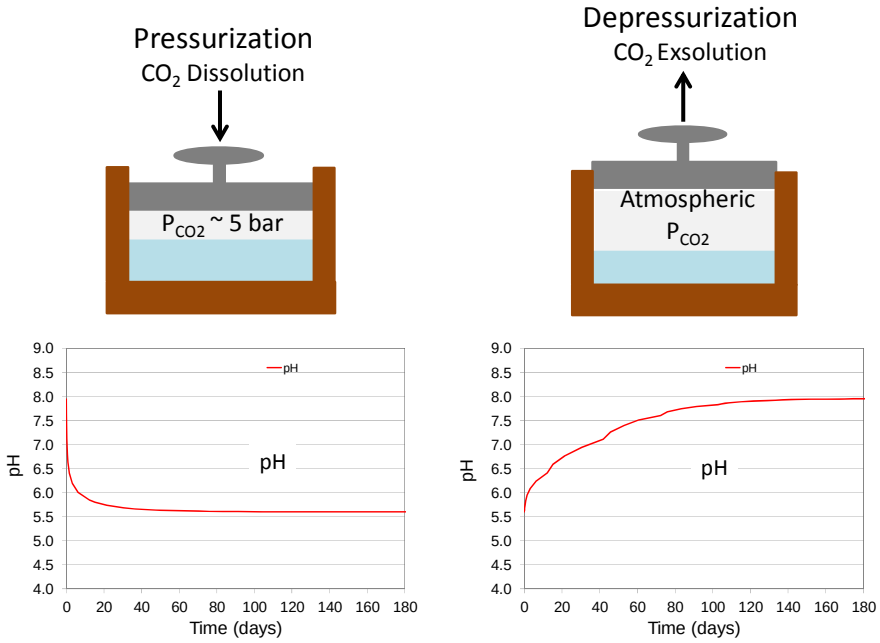

Figure 6. Illustration of numerical experiments of CO_2 pressurization and depressurization, with resulting pH shown (see Appendix B for details on initial conditions).

775